Error field and magnetic diagnostic modeling for W7-X

S.A. Lazerson[1], D.A. Gates[1], H. Neilson[1], M. Otte[2], S. Bozhenkov[2], T.S. Pedersen[2], J. Geiger[2], J. Lore[3]

[1] *Princeton Plasma Physics Laboratory, Princeton, U.S.A.*

[2] *Max-Planck-Institut für Plasmaphysik, Greifswald, Germany*

[3] *Oak Ridge National Laboratory, Oak Ridge, U.S.A*

The prediction, detection, and compensation of error fields for the W7-X device will play a key role in achieving a high beta ($\beta = 5\%$), steady state (30 minute pulse) operating regime utilizing the island divertor system [1]. Additionally, detection and control of the equilibrium magnetic structure in the scrape-off layer will be necessary in the long-pulse campaign as bootstrap current evolution may result in poor edge magnetic structure [2]. An SVD analysis of the magnetic diagnostics set indicates an ability to measure the toroidal current and stored energy, while profile variations go undetected in the magnetic diagnostics. An additional set of magnetic diagnostics is proposed which improves the ability to constrain the equilibrium current and pressure profiles. However, even with the ability to accurately measure equilibrium parameters, the presence of error fields can modify both the plasma response and diverter magnetic field structures in unfavorable ways. Vacuum flux surface mapping experiments allow for direct measurement of these modifications to magnetic structure. The ability to conduct such an experiment is a unique feature of stellarators. The trim coils may then be used to forward model the effect of an applied $n = 1$ error field. This allows the determination of lower limits for the detection of error field amplitude and phase using flux surface mapping. *Research supported by the U.S. DOE under Contract No. DE-AC02-09CH11466 with Princeton University.

Introduction

The measurement, control, and prediction of the edge magnetic structure in W7-X is essential to divertor operation. The island divertor in W7-X utilizes a $5/5$ edge island structure and sophisticated non-axisymmetric baffle plate system. Proper operation of the divertor requires the edge island structure remain intact as beta increases. While a low magnetic shear design helps to achieve this, external error fields and bootstrap currents may rotate or stochasticize this island structure. Furhermore, an $n = 1$ error field could resonantly interact with the $5/5$ edge island structure generating a superimposed stellarator symmetry breaking $n = 1$ edge island. The ability to detect profile variations in real time would allow control systems to adapt to changing plasma currents. The existence of vacuum flux surfaces allows for error field detection and compensation using flux surface mapping techniques. This work explores an improved magnetic

diagnostic set for control and flux surface mapping as an error field measurement mechanism.

An improved magnetic diagnostic set

Real-time determination of pressure and current profiles will be key to the success of the island divertor in the W7-X device. Magnetic diagnostics provide a robust, fast means for the determination of such profile quantities. However, the existing set of magnetic diagnostics on W7-X has been predicted to be mostly insensitive to changes in equilibrium profiles. This motivates the exploration of a new set of magnetic diagnostics sensitive to profile variation. Determination of pressure and current profiles would then allow a plasma control system to measure and react to the predicted changes in bootstrap current.

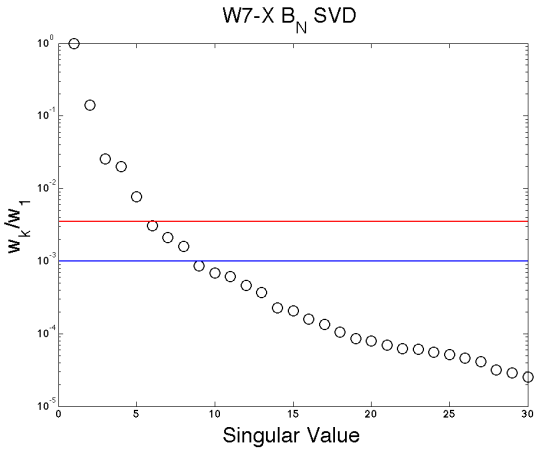

Figure 1: The SVD analysis of the new diagnostic set shows five principle components above the 1 G limit (red) and three more above the accuracy limit (blue) for the magnetic diagnostics calculation.

Building on work developed for the NCSX stellarator [3], a new set of magnetic diagnostics were explored for improved sensitivity to profile variations. The STELLOPT and DIAGNO codes were utilized to explore a set of $\sim$ 8000 VMEC equilibria, evaluating the response of 756 B-normal probes (placed on the vacuum vessel surface). A singular value decomposition of the resulting signal database detected 8 singular values above the signal accuracy limit of 0.1% (Fig. 1). Five of these were above a 1 Gauss threshold.

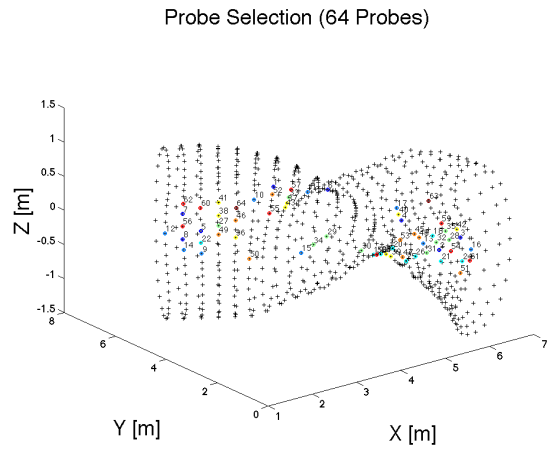

Figure 2: The ranking of first 64 most relevant sensors places them near the bean shaped cross section. Blue dots indicate the most important sensors, red the least.

The Jolliffe's B2 method [4] was utilized to rank the 64 most significant probes in this dataset. This set of probes is localized on the inboard side of the bean shaped cross section (Fig. 2). Here blue dots indicate the greatest significance, red the least. This suggests that a more dense set of probes located in this region be examined as a set of possible future diagnostics. Additionally, poloidal and toroidal field measurements should will be included.

Error field effects on flux surface mapping

The planned flux surface mapping experiments in W7-X allow for the effect of error fields on divertor island structure to be directly measured. In these experiments the unique nature of stellarators (vacuum flux surfaces) is utilized by injection of electron beams into the vacuum field and their resulting scintillation on a phosphorus rod. Given the finite size of the electron beam and detection rod a question arrises as to the minimum detectable effect of error fields in such an experiment. And what effect the trim coils (designed to counteract the effects of error fields) have on the edge island structure themselves.

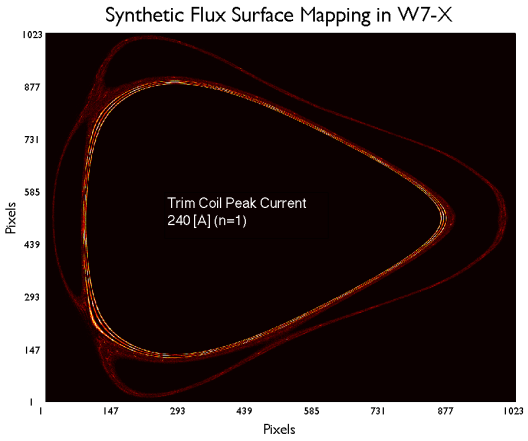

Figure 3: Synthetic flux surface mapping image.

The FIELDLINES code was utilized to follow field lines in the vacuum standard configuration for various trim coils amplitudes and phases. This code uses an adaptive integration method to trace magnetic field lines on a cylindrical grid. It has been parallelized to speed up construction of the vacuum fields and integration of field line trajectories. The trim coils are composed of 5 copper coils located on the exterior of the device. Four of the coils are identical with 48 turns, and the fifth coils has a modified shape with 72 turns [5].

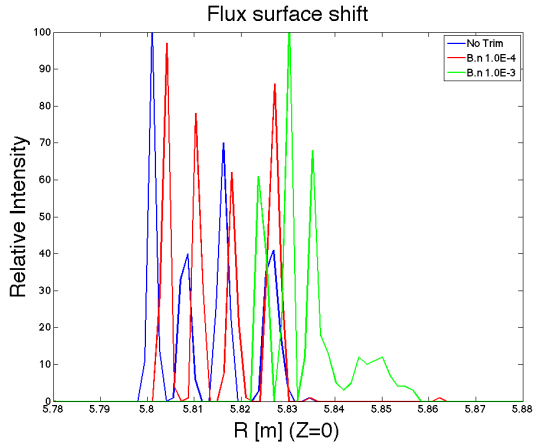

Figure 4: Shift in peak intensity due to applied $n = 1$ error field.

A set of trim coils current were calculated for an $n = 1$ mode and used to evaluate their effect on edge island structure. Using the outboard edge of the plasma (at $\sim 6.25\ m$) as a reference it was found that the trim coils could produce a peak field of ~ 3 Gauss with $\sim 24\ A$ of current. For perspective the coils were designed for peak current of $1.8\ kA$. This low level of error field indicated $\sim 1\ cm$ of strike point asymmetry between field periods. Additionally, an up-down asymmetry was already clearly present in the island structure. Increasing the coil current by a factor of 10 resulted in strike point variation of up to 4 cm from field period to field period. Additionally,

significant edge stochastic fields had formed near many of the upper and lower strike points.

Using the trim coils as a proxy for the error fields, the sensitivity of the flux surface mapping to error fields may be evaluated. To simulate the electron gun the initial location of Poincaré traces of 256 lines were localized to a 1 *mm* radius at the center of the emitter. The emitter location was then scanned across the inboard mid plane of the triangular cross section (toroidal angle of 328^o). The Poincaré plots where the made at the 108^o toroidal plane to approximate the position of the fluorescent rod. The field lines were followed for 1000 toroidal transits. The field lines traces were then binned which acts a proxy for the intensity which will be measured by a CCD camera (Fig. 3). As the amplitude of the applied error field is changed, a clear shift is present in the mapped flux surfaces (Fig. 4). This suggests that so long as ~ 1 cm shifts are detectable, error fields of the order of 5 Gauss should be detectable. The phase of an $n = 1$ error field should also be detectible two detection planes exist on nearly opposite sides of the machine.

References

[1] Geiger J, Wolf R C, Beidler C D, Cardella A, Chlechowitz E, Erckmann V, Gantenbein G, Hathiramani D, Hirsch M, Kasparek W, Kisslinger J, König R, Kornejew P, Laqua H P, Lechte C, Lore J, Lumsdaine A, Maaßberg H, Marushchenko N B, Michel G, Otte M, Peacock A, Sunn Pedersen T, Thumm M, Turkin Y, Werner A, Zhang and the W7-X Team, Plasma Phys. Control. Fusion **55**, 014006 (2013)

[2] Geiger J, Beidler C D, Drevlak M, Maaßberg H, Nührenberg C, Suzuki Y and Turkin Y, Contrib. Plasma Phys. **50**, 770 (2006)

[3] Pomphrey N, Lazarus E A, Zarnstorff M C, Boozer A H, and Brooks A B, Phys. Plasmas **14**, 056103 (2007)

[4] Jolliffe I T, Appl. Stat. **21**, 67 (1972)

[5] Rummel T, Risze K, Fullenbach F, Koppen M, Kisslinger J, Brown T, Hatcher R, Langish S, Mardenfeld M, and Neilson H, IEEE Trans. Appl. Supercond. **24** 4200904 (2014)